EURODYN 2020
XI International Conference on Structural Dynamics
M. Papadrakakis, M. Fragiadakis, C. Papadimitriou (eds.)
Athens, Greece, 22–24 June 2020

MITIGATION OF AMPLIFIED RESPONSE OF RESTRAINED ROCKING WALLS THROUGH HORIZONTAL DAMPERS

Fabio Solarino[1,2]**, Linda Giresini**[1]**, and Daniel V. Oliveira**[2]

[1] Department of Energy, Systems and Territory Engineering (DESTEC)
University of Pisa
Largo Lucio Lazzarino, 1 56126, Pisa (PI), Italy
solarino.fabio@gmail.com, linda.giresini@unipi.it

[2] ISISE, Institute of Science and Innovation for Bio-Sustainability (IB-S), Department of Civil Engineering
University of Minho
Azurém, P-4800-058, Guimarães, Portugal
danvco@civil.uminho.pt

Keywords: Damping, Rocking, Restrained rocking, Non-linear dynamic analysis.

Abstract. *Failure mechanisms in masonry walls are commonly due to the low tensile strength of masonry that could cause overturning or pounding due to the interaction with transverse walls. In this paper, the influence of dissipative devices easing the dynamic stability of rocking blocks is studied considering the main parameters affecting the response. Normalized rotation time-histories are obtained for six geometrical configurations under several acceleration records in order to analyse possible resonant effects and beneficial reductions due to the presence of a damper, accounted for in the equation of motion of the one-sided restrained rocking block. Rocking response spectra obtained for undamped systems show that possible beat phenomena may arise for certain geometrical configurations and restraint stiffness values. A design equation for the damping coefficient is proposed for the anti-seismic device and its influence in the response is also analysed in terms of energy dissipation over the oscillations.*

1 INTRODUCTION

Recent seismic events demonstrated that out-of-plane mechanisms are commonly developed in historical masonry constructions causing relevant cracks and sometimes leading to catastrophic collapses. This can be due to not proper wall-to-diaphragm connections (Solarino, Oliveira, and Giresini 2019) or to slender walls as those of church façades (Argiento, Maione, and Giresini 2019; Casapulla, Giresini, et al. 2019; Casapulla, Argiento, and Maione 2018; Casapulla, Jossa, and Maione 2010). Portions of the building can tilt as rigid blocks around plastic hinges developed during earthquakes, even of low entity, involving complex phenomena of friction, impact, sliding and possible overturning (Casapulla 2001; Ishiyama 1982). The most significant way to treat these problems, due to the many uncertainties that affect them, is a probabilistic approach considering univariate and bivariate fragility curves (L. Giresini et al. 2018; Giresini, Taddei, et al. 2019).

Kinematic approach is considered one of the most valid tools for the assessment of local modes, based on the assumption of the "most probable" mechanisms that can be developed during a seismic event. This method is widely used worldwide and the Italian national code (D.M. 17/01/2018 2018) suggests that approach for the verification of local mechanisms, necessary for successive global assessment. Besides more complex models can account for horizontal restraints or frictions, the method is based on the pseudo-static application of virtual work principle, thus setting the limit of the approach.

Recent developments were done on rocking analysis, capable of assessing the dynamic stability of rigid restrained blocks and suitable to understand the behavior of the tilting object during the motion (Argiento et al. 2019; Casapulla, Maione, and Argiento 2019; Giresini, Solarino, et al. 2019). Newly published national Italian standard [NTC2018] (D.M. 17/01/2018 2018; Ministero delle infrastrutture e dei trasporti 2019) allows the assessment of local mechanisms through the use of nonlinear dynamic analysis of rigid bodies. During the oscillation of rocking structures, the seismic energy is dissipated through the impacts and this can be accounted for in the equation of motion through a coefficient of restitution, whose experimental estimation is of crucial relevance (Linda Giresini, Sassu, and Sorrentino 2018). The rocking block can be free-standing, namely without restraints (Makris and Konstantinidis 2003) or with vertical (Makris and Vassiliou 2015) or horizontal (Giresini 2017) elastic restraints. If a further source of energy dissipation is desired, to control the stability of the rocking wall, the restraint could be characterized by a viscous-elastic damper.

In this contribution, a damper device is intended to be designed in order to control possible damages occurring on out-of-plane masonry walls. This paper aims at understanding the influence of damping and stiffness of anti-seismic devices through rocking analysis.

2 EQUATION OF MOTION AND RESONANCE CONDITION

The full equation of motion of a damped restrained rocking block in one-side motion under seismic force reads:

$$I_0\ddot{\theta} + sign(\theta)mgR\sin A_\theta + T_K + T_{K'} + T_D = m\ddot{u}_g R\cos A_\theta, \qquad (1)$$

where, I_0 is the polar moment of inertia of the block with mass m oscillating about the pivot points O and O' of an angle θ, R is the semi-diagonal of the block and $A_\theta = \alpha - sign(\theta)\backslash theta,$ in which α is the angle between the direction of R and the vertical, being also the inverse of the slenderness of the block ($\alpha = \tan^{-1}\left(\frac{s}{h}\right) \sim \frac{s}{h} = 1/\lambda$).

The term T_K relates to the contribution of a horizontal spring, referring to the elastic stiffness of the damper or to separate restraints (steel ties). For the scope of this work the pre-tensioning and yielding

are not considered, being the spring indefinitely linear elastic characterized by certain axial stiffness, K, whose term reads:

$$T_K = sign(\theta) K R_t^2 \cos A_t \left(sin\alpha_r - sinA_{r,\theta}\right),$$

where $A_t = \alpha_t - sign(\theta)\,\theta$ and geometrical parameters R_t and α_t define the position of the spring.
The term Td depends upon the damping, c, and the relative velocity between the damper ends, $\dot{\theta}$, and reads:

$$T_d = cR_d^2 \cos^2 A_{d,\theta}\dot{\theta},$$

Where $A_d = \alpha_d - sign(\theta)\,\theta$ and, at the same way of horizontal spring, R_d and α_d define the position of the damper.
It can be noted that the sign of damping term is directly given by the sign of rotational velocity, $\dot{\vartheta}$, thus no $sign$ function is necessary in this case.

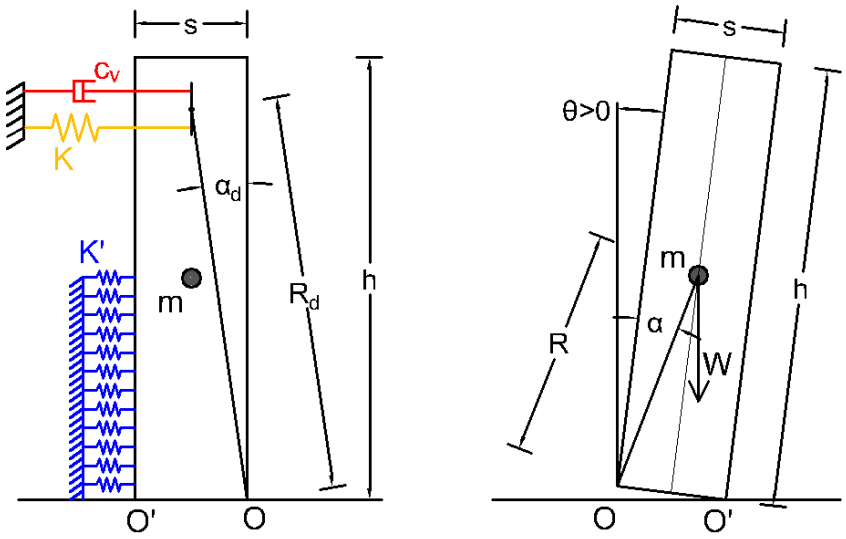

Figure 1: Rocking block model restrained by damper and elastic spring in one-sided motion: geometry and definition of positive rotation

Previous studies demonstrated that amplified response can be achieved in certain circumstances associated with resonance condition (Giresini 2017 – EURODYN2017). Depending on the direction of motion, two rocking systems can be defined, one referring to clockwise rotation (single spring in tension) and the other to counterclockwise direction (spring bed in compression). Thus, ideal values of resonance frequencies can be computed for both systems,

$$\omega_r^+ = p\sqrt{\left(\frac{K\beta^2 R}{mg} - 1\right)}$$

and

$$\omega_r^- = p\sqrt{\left(\frac{8K_c' R^2}{3mg} - 1\right)}$$

Even if circular frequency of the rocking system varies during the oscillation, it was seen that the horizontal elastic restraint behaves like a “filter” for the output signal. This aspect is confirmed in Figure 2 showing the comparison between the fast fourier transform (FFT) of the displacement response in restrained and in free-standing configuration, under free vibration. The restrained configuration is

defined, here, by the presence of a bidirectional indefinitely linear elastic tie with stiffness equal to K = 1.0e6 N/m.

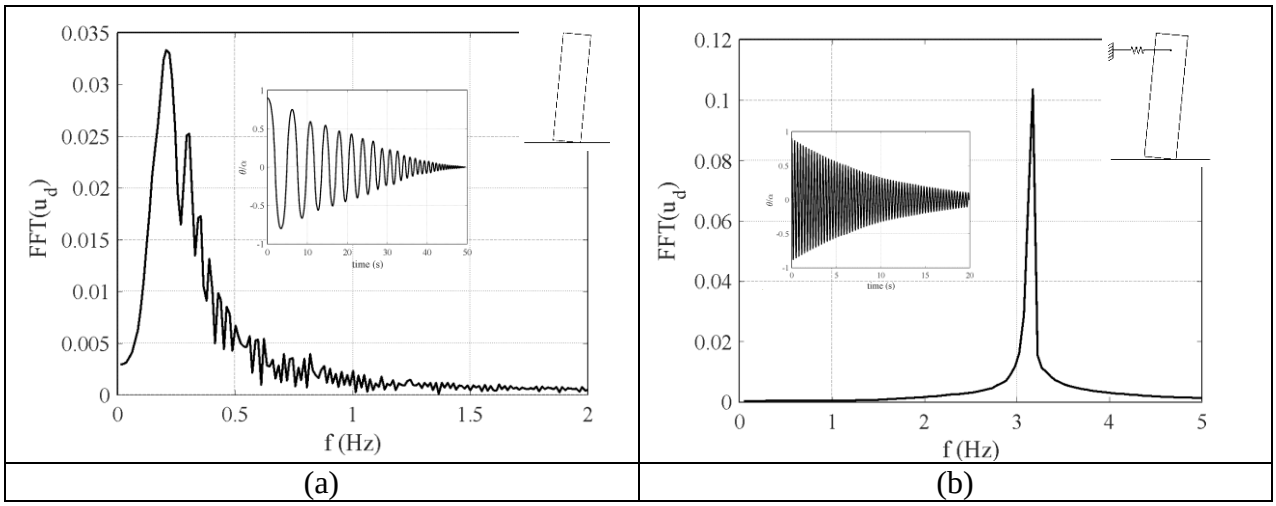

Figure 2: Fast fourier transform of horizontal displacement read at the level of restraint; (a) free-standing block; (b) restrained block

The restrained rocking block response is characterized by a reduced frequency content if compared to the free-standing configuration. Ideally, if such a restrained system is forced by excitations with similar frequencies, dangerous amplified responses may arise and should be controlled. Artificial inputs with similar frequency content have been adopted in recent studies in order to cause resonant response (Giresini et al. 2020 - EESD). In this paper, possible resonance circumstances are investigated under real ground motion, which are characterized by a complex frequency content but representative of realistic situations.

3 GEOMETRIES AND HYPOTHESIS

label	lambda	s [m]	h [m]	m [kg]	R [m]	I_0 [kg*m2]
block 1	10	0.3	3	1926.606	1.5074813	5837.614679
block 2	10	0.6	6	7706.422	3.0149627	93401.83486
block 3	10	0.9	9	17339.45	4.522444	472846.789
block 4	13	0.3	3.9	2504.587	1.9557607	12773.3945
block 5	13	0.6	7.8	10018.35	3.9115214	204374.3119
block 6	13	0.9	11.7	22541.28	5.8672822	1034644.954

Geometries of unit length were selected in order to study two different slenderness ratios ($\lambda = 10, 13$) and three different wall thickness values ($s = 0.3, 0.6$ and $0.9\ m$), resulting in a total of six geometrical

layouts representative of common masonry wall façades. The masonry weight density was assumed equal to 21 kN/m^3 for all blocks. The analysis of damped restrained rocking blocks requires the definition of the horizontal restraint elastic stiffness, representing a possible steel tie rod placed at a certain height of the wall. Moreover, for the definition of the elastic impact with transverse walls, a value of stiffness (per unit length) needs to be set. A realistic value of K' can be based on thickness, t, and effective width, L_{eff}, of certain transversal walls with equivalent lateral elastic modulus, E_x,

$$K' = E_x\, t/L_{eff},$$

If the system global stiffness in the positive direction equates the ones in negative direction (Giresini 2017 - COMPDYN 2017), the spring bed stiffness becomes a function of horizontal restraint stiffness:

$$K_{sys} = K'_{sys} \rightarrow K'_c = K\frac{3}{8}\frac{\beta^2}{Rcos(\alpha)}\ .$$

A reference value of tie stiffness, K_d, can be calculated starting from a design value of steel tie rod diameter, ϕ_d, based on simple equilibrium criterium (equation []), assuming the seismic action as a horizontal equivalent static force acting at the center of gravity of the block. The length of the tie rod is assumed to be 10 m.

$$T_d h_t + \frac{Ws}{2} = \frac{\mu W h}{2},$$

were $T_d = \frac{\sigma_d \pi \phi_d^2}{4}$ is the force given by the tie, applied at height h_t , computed considering a steel (S275) design stress value, $\sigma_d = \frac{0.7 f_{uk}}{1.05}$, W is the self weight of the block and $\mu = 0.2$ is the collapse multiplier. Even if it is hard to define a critical damping for rocking blocks (appropriate for single-degree-of-freedom oscillators), mainly because of the non-constant value of eigenfrequency (Housner), a reference value of damping can be defined starting from the capacity curve of the free-standing block. The damping becomes function of the solely geometry of the block and a characteristic event time, Δ_t (Giresini et al. 2020 - EESD):

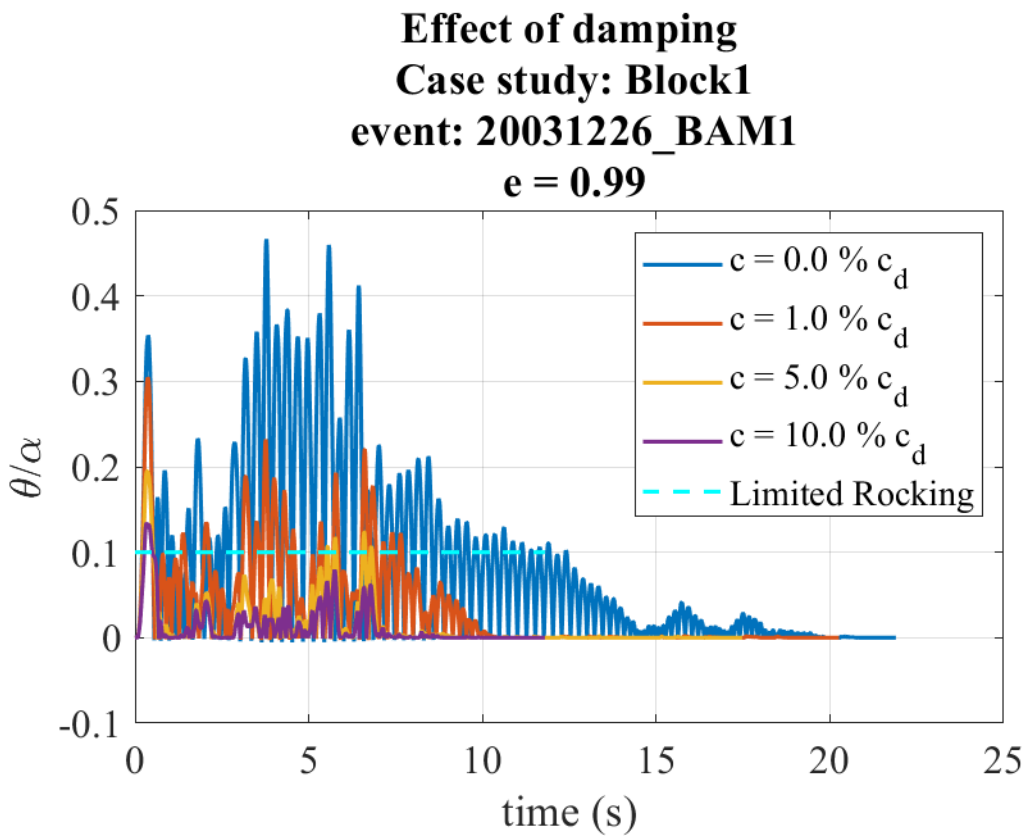

$$c_d = \frac{F_0}{v} = \frac{\lambda \cdot W}{\Delta u / \Delta t} = 2 \cdot W/h \cdot \Delta t = 2\frac{m \cdot g}{h}\Delta t \qquad (16)$$

The viscous-elastic damper, which is ruled by a stiffness K and a coefficient of damping c, is located at the top of the wall. Furthermore, dampers are ideally bilinear.
It is worth noting that the yielding of the steel tie rod was not considered, as outer the scope of the study.

4 ANALYSIS AND RESULTS

The influence of the wall geometries and of the viscous-elastic damper on the dynamic stability of rocking walls are studied under free and forced vibration in one-sided motion. For the latter analyses, a selection of several (> 40) real accelerograms was done in order to consider a wide range of frequency content and intensity levels. Strong motion accelerations are selected among recent seismic events that stroke Central Italy during 2016 - 2017 and past events characterized by high level of magnitude (i.e. M_w > 5.0). Two limit states are defined for the scope of these analyses as reference values of moderate (ϑ/α = 0.4) and limited (ϑ/α = 0.1) rocking.
aggiungerei un minimo di tabella con dati basici, tanto lo spazio c'è fino a una ventina di pagine...

4.1 Undamped rocking response spectra

The construction of design response spectra is common in civil engineering with the aim of defining the seismic input of a given structure (Makris and Konstantinidis 2003). This method is valid for structures that may be related to classical single degree of freedom (SDOF) systems for which an equivalent period can be defined. Commonly, 5% of damping ratio is considered to take into account the capability of the building on dissipating energy.

Even if rocking systems are characterized by an amplitude-dependent eigen frequency, a rocking spectrum can be defined for a given geometry evaluating the maximum response in terms of normalized rotations under a certain seismic event, for different values of horizontal restraint stiffness. Figure 3 shows the rocking spectrum obtained for the undamped restrained rocking block 2 in one-sided motion (K and K' calculated according to eq. [] in Section 3) under 1995/10/01 6.2 Mw earthquake that struck the municipality of Dinar (Turkey). 50 values of K were chosen within the range of $0 \leq K \leq K\_d$. A limit state of moderate rocking was considered corresponding to $\theta/\alpha = 0.4$ (Casapulla, Giresini, Argiento, Maione 2019).

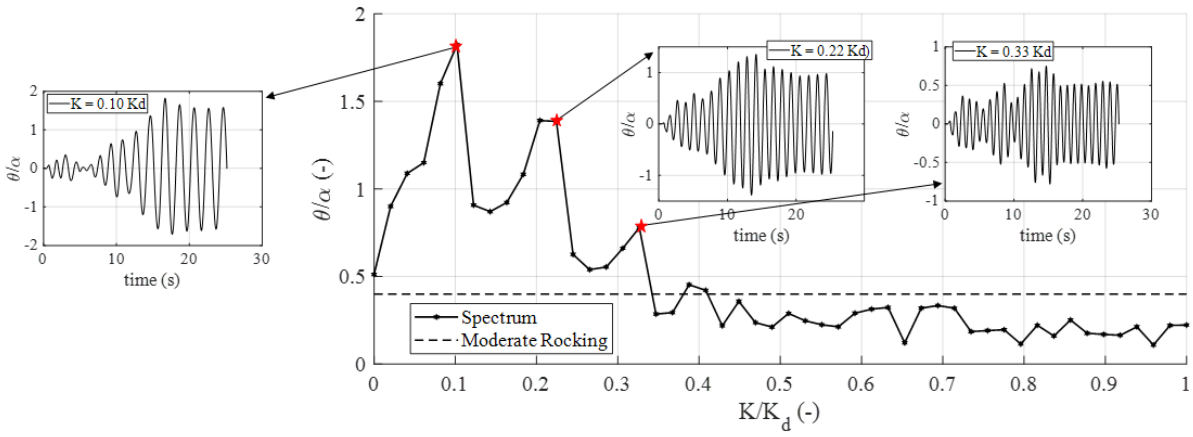

Figure 3: Rocking spectrum obtained for restrained block 2 in one-sided motion under 1995/10/01 Dinar (Turkey) 6.2 Mw earthquake

Amplifications are clearly visible for different values of K where beats and resonant effects develop (Figure 3). This not monotonic trend observed when the stiffness monotonically increases or decreases suggests near-resonance conditions. Response time-histories are shown upon the corresponding spectrum peaks (Figure 4). Even if values of K different from zero should correspond to a more stable response (since the block is ideally "more restrained"), the peaks on the rocking spectrum demonstrate the opposite. Indeed, as shown in Figure 4a, even low values of stiffness result in an amplification of response up to three times. It is worth noting that higher rotations are obtained in few cases for the restrained block (e.g. K = 0.49 Kd) if compared to the free standing configuration (K = 0.0) (Figure 4), meaning that strengthening solutions with elastic devices must be considered with care. In particular, the rocking spectra are therefore recommended in the design of whatsoever horizontal restraint for rocking walls to avoid such undesired amplifications.

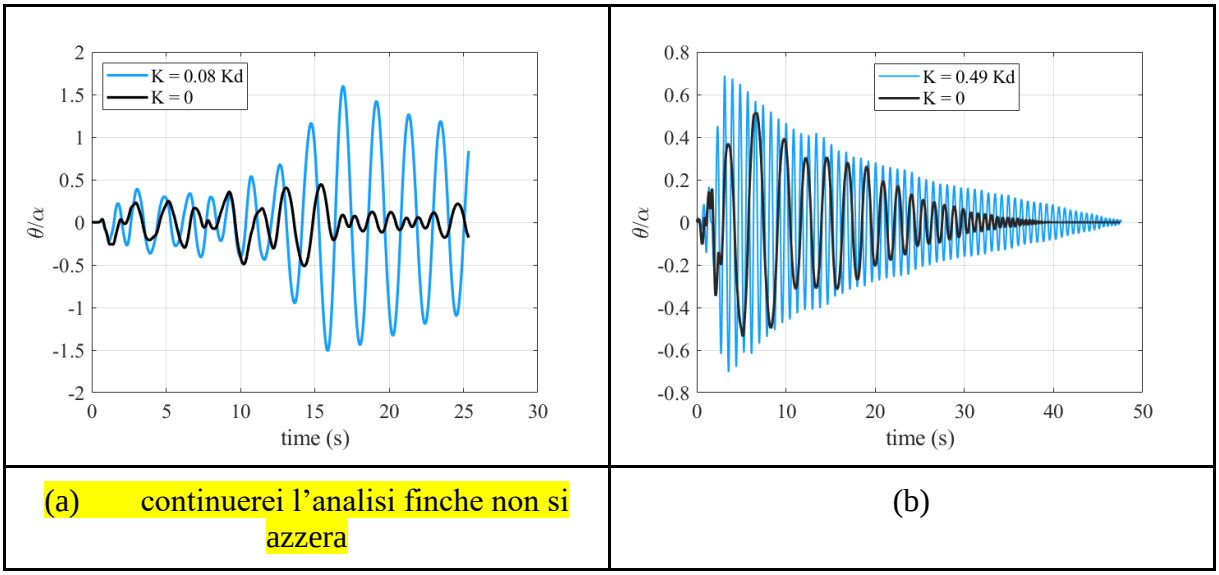

(a) continuerei l'analisi finche non si azzera

(b)

Figure 4: Comparison between free and restrained rocking block responses; (a) block 2 - 1995/10/01-6.2Mw-Dinar earthquake; (b) block 2 - 2016/10/30-6.5Mw-Norcia earthquake

Another result is shown in Figure 5 for block 2 under 2016/10/30-6.5 Mw-Norcia earthquake. The maximum rotations are lower than the moderate rocking limit state only for stiffness values ranging between 0.02<K<0.3, while amplified responses are obtained elsewhere.

Moreover, higher rotations are obtained for restrained configuration if compared with the free-standing configuration, as clear from the first part of the rocking spectrum.

Based on all analyses done, certain geometries results in such resonant phenomena then others, depending on slenderness and inertia values: […]

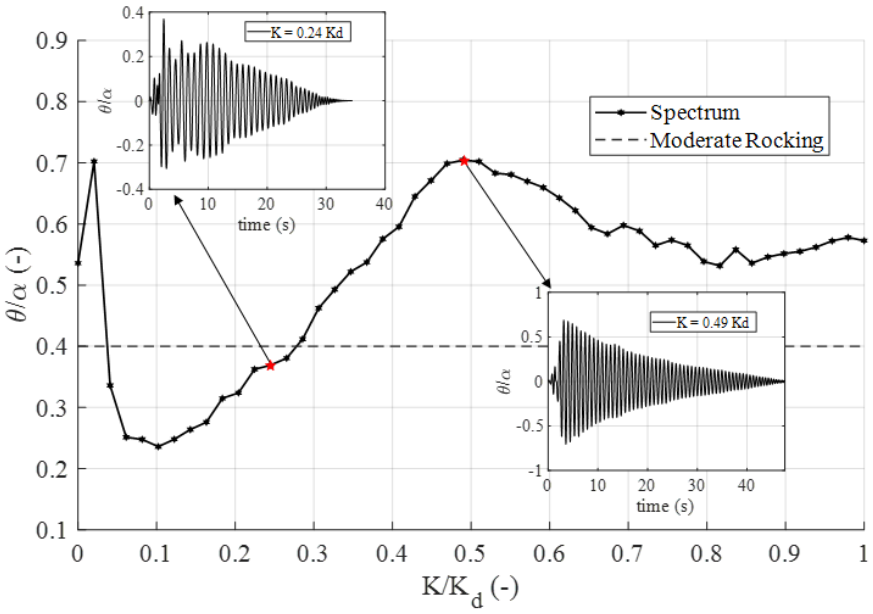

Figure 5: Rocking spectrum obtained for restrained block 2 in one-sided motion under 2016/10/30-6.5 Mw-Norcia

4.2 Damped free vibrations

To better study the influence of damping in the rocking stability of rigid blocks, preliminary analyses are performed on block 1 under free vibrations. For this purpose, an initial normalized rotation, theta/alpha_0 is set equal to 0.9, corresponding to the 90% of the ultimate kinematic displacement capacity (u_g = s/2). Moreover, in order to isolate the influence of viscous damping, a unit value of restitution coefficient is set (e = 1.0), corresponding to perfectly elastic impacts. Firstly, responses under two-sided motion are computed. Secondly, a realistic value of K' is set in order to simulate the presence of transversal walls under both free- and restrained configuration (K = 0.0, and K = K_d, respectively) (Giresini 2017 - COMPDYN).

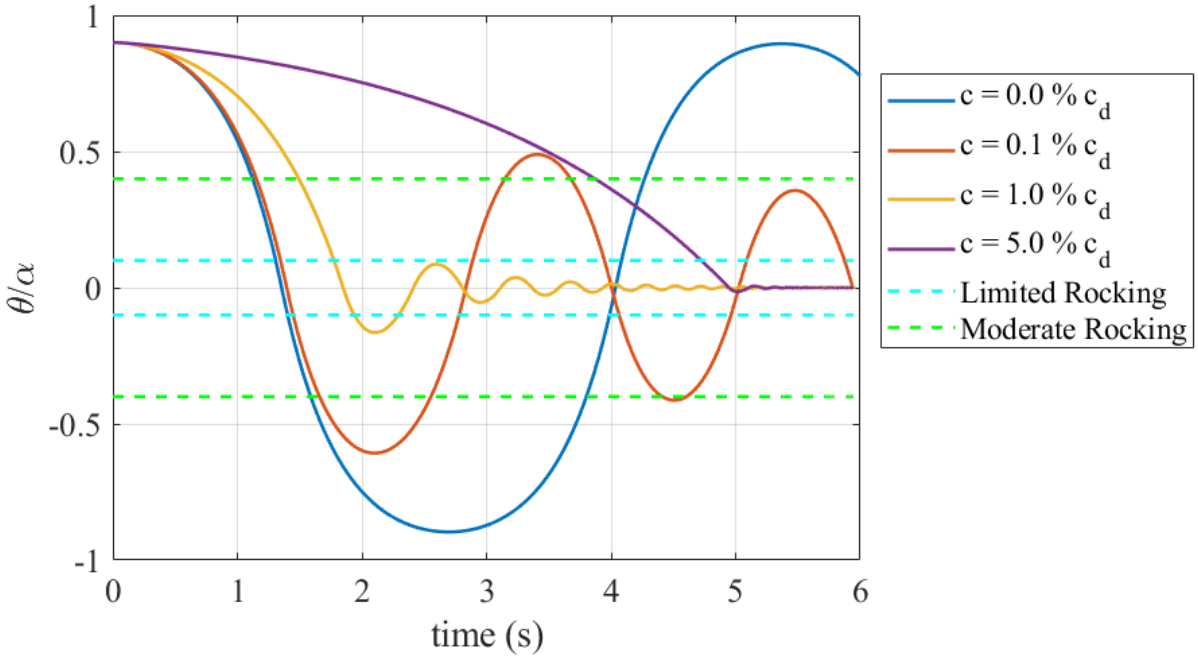

Figure 6: Influence of damping on free-standing rocking block 1 under free vibration in two-sided motion

Assuming the clockwise direction as the positive rotation (Figure 1), the damping contribution is positive for positive rotational velocity, $\dot{\vartheta}$ (Figure 6), coherent with the self weight term, among the others. The sign and the shape of T_d term is validated using the previous block 1 configuration using $c = 0.1\%c_d$.

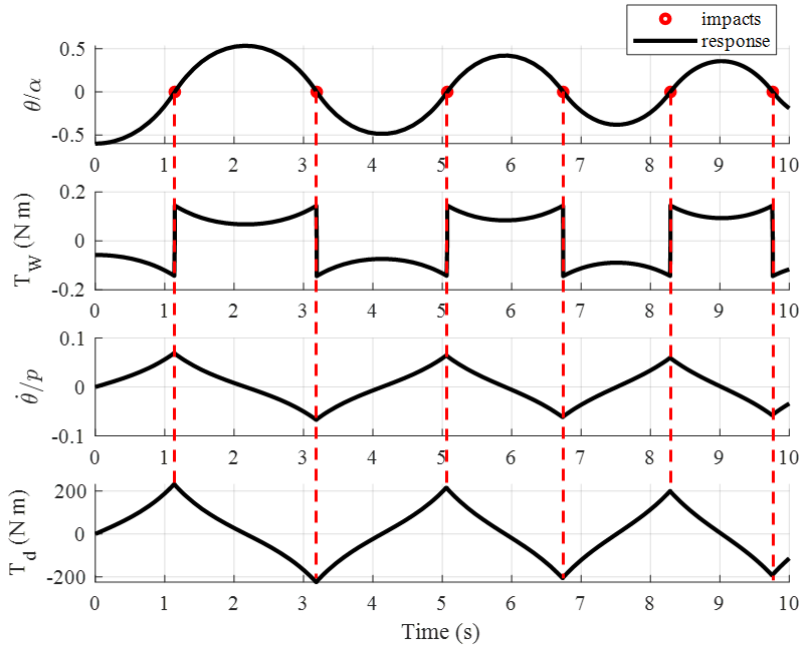

Figure 7: Validation of damping term sign for a simple free vibration time-history analysis of free-standing block 1 in two-sided motion (K=K'=0); from top to bottom: (i) normalized rotation; (ii) self weight term; (iii) normalized rotational velocity; (iv) damping term; (b) damping relative energy

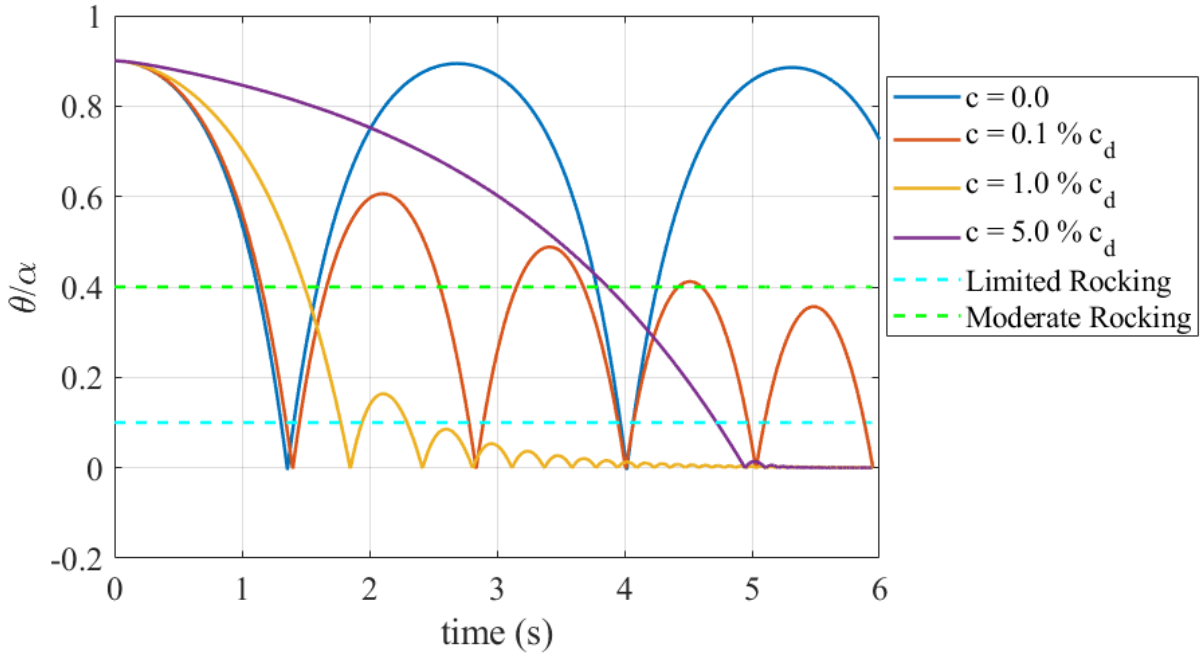

Figure 8: Influence of damping on free-standing (K=0.0) rocking block 1 under free vibration in one-sided motion ($K' \neq 0.0$)

Figure 6 and 8 show the influence of four different values of damping ($c = 0.0, 0.1, 1.0$ and $5.0\ \%\ c_d$) on the damped free-standing block 1 under two- and one-sided motion, respectively (i.e. without and with the presence of transversal walls with equivalent spring bed stiffness K' = 4.5e8 N/m/m, (Giresini COMPDYN 2017). The beneficial effect of increased damping coefficient is clearly visible from the Figures. The damping device decreases the successive peaks and delayed the first impact time, as evidently demonstrated passing from $c = 1\%$ to $c = 5\%\ c_d$.

The effect of dampers is also studied for the restrained configuration (that is with K different from zero), in one-sided motion setting $K = K_d$ as defined in Section 3.

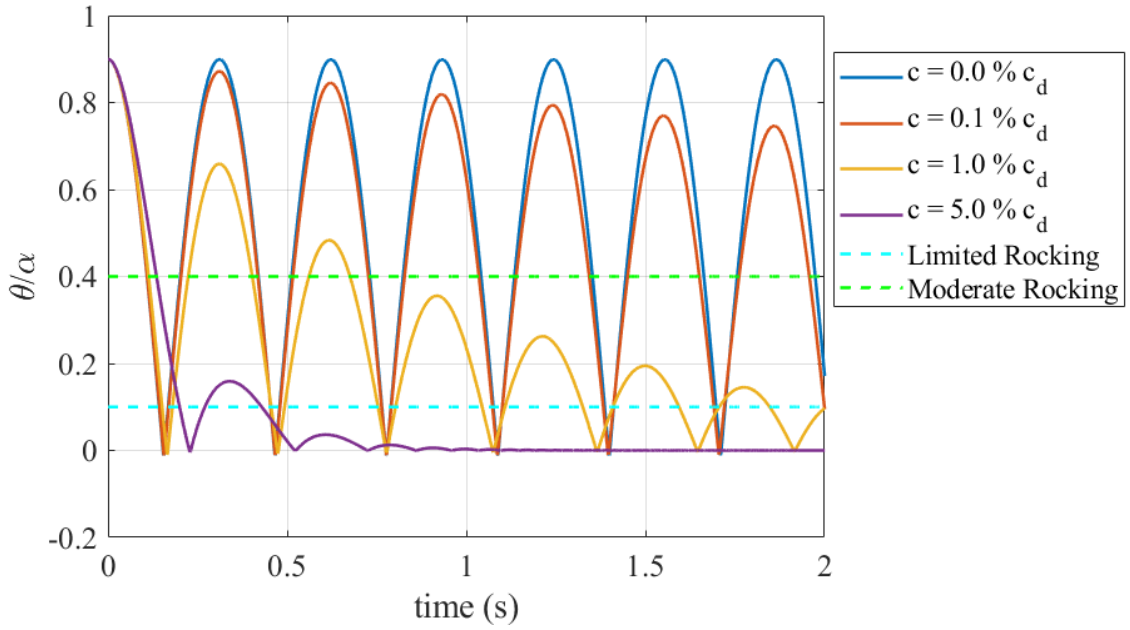

Figure 9: Influence of damping on restrained rocking block 1 under free vibration in one-sided motion

The first impact time is strongly reduced by the presence of the tie re-centering the block in its "zero" position (Figure 8). It is visible an increased rotational frequency due to the restrained condition. This aspect could be problematic in terms of repeated cyclic stresses on the transverse walls, where masonry could crush for the attainment of compressive strength. It is interesting to note that, for the same value of damping coefficient, despite the more "regular" response if compared to the free-standing configuration, higher normalized rotations are obtained for the restrained block. Indeed, as shown in Figure 9, setting c = 1.0 % c_d, the peak reduction is gradual for the restrained block, only corresponding to 27% reduction after the first impact, while a reduction of 82% of normalized rotation is obtained for the free-standing block.

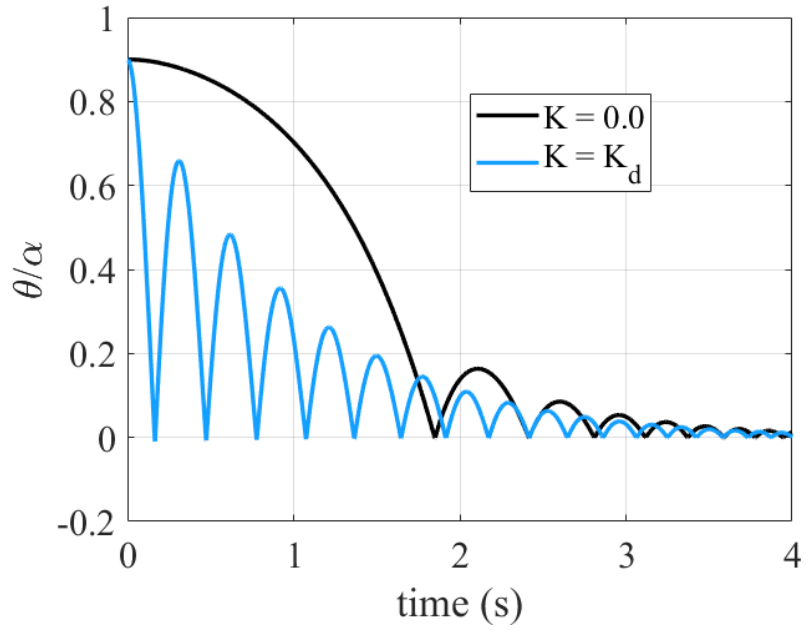

Figure 10: Comparison between free and restrained configuration under free damped vibration in one-sided motion; block 1, c = 1%c_d

4.3 Damped forced vibrations

Nonlinear analyses of the restrained ($K = K_d$) blocks with same geometries are performed under real inputs in order to study the influence of damping. The lateral stiffness per unit length is computed according to Equation []. For the purpose of this work, a value of $E_x = 1.5e9\ N/m/m$ can be used according to C8A.2.1 circ. 2019 NTC2008. Moreover, 30 cm thickness and 1.0 m length can be assumed.

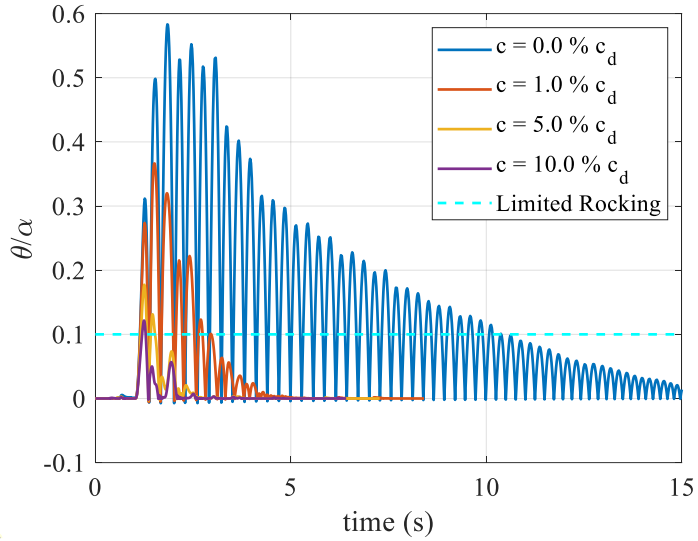

Figure 11: Influence of damping on restrained block 1 under 2016/10/26-5.4 Mw-Visso earthquake

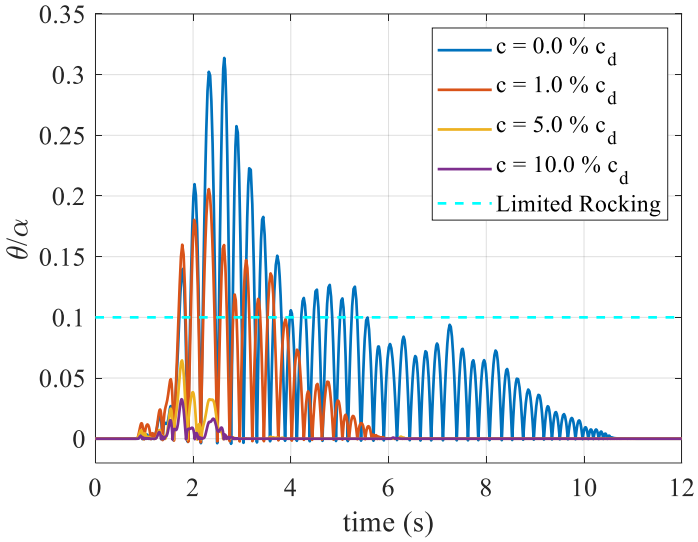

Figure 12: Influence of damping on restrained block 1 under 2016/08/24-6.0 Mw-Accumoli (RI) earthquake

The beneficial effect of damping is clear in Figures 11 and 12 where a significant reduction of maximum normalized rotation is obtained for higher values of damping. Figure 11 also shows that amplified response is obtained for the undamped case characterized by high and relatively long oscillations probably caused by the bouncing and near resonant effects given by the tie. The rotation time-history shape is similar during the first impacts only, as successive frequency and peaks values are affected by damping force. Besides the response is strongly dependent on the geometry of the block and the type of input, damping values of c > 10% cd should fulfill the limited rocking limit state.

5 CONCLUSIONS

This paper analyzed the dynamic response of out-of-plane rocking walls with a viscous-elastic damper at the top under recorded acceleration time histories. Six different geometries were tested to investigate the role of size and slenderness of the rigid block in the dynamic response. From the non-linear analyses outcomes, a not monotonic trend in rocking spectra was observed when the stiffness was monotonically increased or decreased. The rocking spectra are therefore recommended in the design of whatsoever

horizontal restraint for rocking walls to avoid such undesired amplifications due to near-resonance conditions. Moreover, the influence of damping was investigated in free and forced vibrations. As for the response in free vibrations, the beneficial effect of a greater damping coefficient was clearly visible, since it caused a reduction of consecutive peaks and delayed the first impact time. The effect of dampers was also studied for the restrained configuration in one-sided motion. The first impact time was strongly reduced by the presence of the tie that re-centered the block in its "zero" position. Moreover, the resulting increased rotational frequency due to the restrained condition could be problematic in terms of repeated cyclic stresses on the transverse walls, where masonry could crush for the attainment of compressive strength. Forced vibrations responses also results in advantageous use of damper devices for the control of rocking motion of walls, considered in a realistic one-sided configuration sensitive to possible resonant behaviors. Not only maximum normalized rotations are strongly reduced by higher values of damping, but responses time-histories present relevant changes in terms of frequency and shape after the first impacts. A value of $c > 10\%$ can be evaluated as the corresponding design value for the limited rocking limit state, but further analyses are necessary and intended in order to account for geometries and several inputs.

REFERENCES

Argiento, Luca Umberto, Alessandra Maione, and Linda Giresini. 2019. "The Corner Failure in a Masonry Building Damaged by the 2016-2017 Central Italy Earthquake Sequence." Pp. 633–50 in *COMPDYN 2019 7th ECCOMAS Thematic Conference on Computational Methods in Structural Dynamics and Earthquake Engineering*. Crete; Greece; 24th-26th June 2019.

Casapulla, Claudia. 2001. "Dry Rigid Block Masonry: Safe Solutions in Presence of Coulomb Friction." *WIT Transactions on the Built Environment* 55:251–61.

Casapulla, Claudia, Luca Umberto Argiento, and Alessandra Maione. 2018. "Seismic Safety Assessment of a Masonry Building According to Italian Guidelines on Cultural Heritage: Simplified Mechanical-Based Approach and Pushover Analysis." *Bulletin of Earthquake Engineering* 16(7):2809–37.

Casapulla, Claudia, Linda Giresini, Luca Umberto Argiento, and Alessandra Maione. 2019. "Nonlinear Static and Dynamic Analysis of Rocking Masonry Corners Using Rigid Macro-Block Modeling." *International Journal of Structural Stability and Dynamics* 19(11):1950137.

Casapulla, Claudia, P. Jossa, and A. Maione. 2010. "Rocking Motion of a Masonry Rigid Block under Seismic Actions: A New Strategy Based on the Progressive Correction of the Resonance Response." *Ingegneria Sismica* 27(4):35–48.

Casapulla, Claudia, Alessandra Maione, and Luca Umberto Argiento. 2019. "Performance-Based Seismic Analysis of Rocking Masonry Façades Using Non-Linear Kinematics with Frictional Resistances: A Case Study." *International Journal of Architectural Heritage*.

D.M. 17/01/2018. 2018. "Aggiornamento Delle 'Norme Tecniche per Le Costruzioni' (in Italian)."

Giresini, L., C. Casapulla, R. Denysiuk, J. Matos, and M. Sassu. 2018. "Fragility Curves for Free and Restrained Rocking Masonry Façades in One-Sided Motion." *Engineering Structures* 164:195–213.

Giresini, L., F. Solarino, O. Paganelli, D. V. Oliveira, and M. Froli. 2019. "One-Sided Rocking Analysis of Corner Mechanisms in Masonry Structures: Influence of Geometry, Energy Dissipation, Boundary Conditions." *Soil Dynamics and Earthquake Engineering* 123:357–70.

Giresini, Linda. 2017. "Design Strategy for the Rocking Stability of Horizontally Restrained Masonry Walls." in *COMPDYN 2017 6th ECCOMAS Thematic Conference on Computational Methods in Structural Dynamics and Earthquake Engineering*, edited by M. F. M. Papadrakakis. Rhodes Island, Greece.

Giresini, Linda, Mauro Sassu, and Luigi Sorrentino. 2018. “In Situ Free-Vibration Tests on Unrestrained and Restrained Rocking Masonry Walls.” *Earthquake Engineering & Structural Dynamics* 47(15):3006–25.

Giresini, Linda, Francesca Taddei, Claudia Casapulla, and Gerhard Mueller. 2019. “Stochastic Assessment of Rocking Masonry Façades under Real Seismic Records.” Pp. 673–89 in *COMPDYN 2019 7th ECCOMAS Thematic Conference on Computational Methods in Structural Dynamics and Earthquake Engineering*. Crete; Greece; 24th-26th June 2019.

Ishiyama, Y. 1982. “{M}otions of Rigid Bodies and Criteria for Overturning by Earthquake Excitations.” *Earthquake Engineering and Structural Dynamics* 10:635–50.

Makris, Nicos and Dimitrios Konstantinidis. 2003. “The Rocking Spectrum and the Limitations of Practical Design Methodologies.” *Earthquake Engineering and Structural Dynamics* 32(2):265–89.

Makris, Nicos and Michalis F. Vassiliou. 2015. “Dynamics of the Rocking Frame with Vertical Restrainers.” *Journal of Structural Engineering* 141(10).

Ministero delle infrastrutture e dei trasporti. 2019. *Circolare Applicativa 21 Gennaio 2019, n. 7*.

Solarino, Fabio, Daniel Oliveira, and Linda Giresini. 2019. “Wall-to-Horizontal Diaphragm Connections in Historical Buildings: A State-of-the-Art Review.” *Engineering Structures* 199.